CANCER
LETTERS

Original Articles

Dehydroleucodine inhibits tumor growth in a preclinical melanoma model by inducing cell cycle arrest, senescence and apoptosis

CrossMark

Valeria V. Costantino [a], Lorena Lobos-Gonzalez [b], Jorge Ibañez [a], Dario Fernandez [a], F. Darío Cuello-Carrión [c], Manuel A. Valenzuela [b], Manuel A. Barbieri [d], Silvana N. Semino [a], Graciela A. Jahn [c], Andrew F.G. Quest [b,*], Luis A. Lopez [a,**]

[a] Laboratory of Cell Cycle and Cytoskeleton, Instituto de Histología y Embriología Dr. M. H. Burgos (IHEM-CONICET, Mendoza, Argentina
[b] Cellular Communication Laboratory, Center for Molecular Studies of the Cell (CEMC), Advanced Center for Chronic Diseases (ACCDiS), Program of Cell and Molecular Biology, Institute of Biomedical Sciences (ICBM), School of Medicine, Universidad de Chile, Santiago 8380453, Chile
[c] Instituto de Medicina y Biología Experimental de Cuyo IMBECU-CONICET, Mendoza, Argentina
[d] Department of Biological Sciences, Florida International University, Miami, FL 33199, USA

ARTICLE INFO

ABSTRACT

Malignant melanoma represents the fastest growing public health risk of all cancer types worldwide. Several strategies and anti-cancer drugs have been used in an effort to improve treatments, but the development of resistance to anti-neoplastic drugs remains the major cause of chemotherapy failure in melanomas. Previously, we showed that the sesquiterpene lactone, dehydroleucodine (DhL), promotes the accumulation of DNA damage markers, such as H2AX and 53BP1, in human tumor cells. Also DhL was shown to trigger either cell senescence or apoptosis in a concentration-dependent manner in HeLa and MCF7 cells. Here, we evaluated the effects of DhL on B16F0 mouse melanoma cells in vitro and in a pre-clinical melanoma model. DhL inhibited the proliferation of B16F0 cells by inducing senescence or apoptosis in a concentration-dependent manner. Also, DhL reduced the expression of the cell cycle proteins cyclin D1 and B1 and the inhibitor of apoptosis protein, survivin. In melanomas generated by subcutaneous injection of B16F0 cells into C57/BL6 mice, the treatment with 20 mg DhL /Kg/day in preventive, simultaneous and therapeutic protocols reduced tumor volumes by 70%, 60% and 50%, respectively. DhL treatments reduced the number of proliferating, while increasing the number of senescent and apoptotic tumor cells. To estimate the long-term effects of DhL, a mathematical model was applied to fit experimental data. Extrapolation beyond experimental time points revealed that DhL administration following preventive and therapeutic protocols is predicted to be more effective than simultaneous treatments with DhL in restricting tumor growth.

Introduction

Sesquiterpene lactones (SLs) are a large and structurally diverse group of plant metabolites, which includes many members with anti-tumor effects, and one of these has been shown to reduce rat melanoma growth [1]. SLs of the guaianolide group are of particular interest as anti-tumor agents because each chemical substitution to the guaianolide skeleton confers a distinct biological activity to the resulting compound [2].Our group is particularly interested in the lactone, dehydroleucodine (DhL), a SL of the guaianolide group

with an alpha-methylene butyrogamma-ring connected to a seven-atom ring that is fused to another exocyclic alpha, beta-unsaturated cyclopentenone ring (for structure see [3] and Fig. 1).

DhL can be isolated and purified to concentrations over 1%, starting from the above-ground parts of Artemisia douglasiana (Besser), a widespread and readily available medicinal herb that is commonly used in Argentina [4]. In a recent study [5], we demonstrated the anti-proliferative effects in vitro of DhL in human cancer cells. Our analysis of the accumulation of DNA damage response (DDR) markers revealed a striking correlation between the extent of DNA damage and the activation of senescence and apoptosis programs, which were selectively stimulated by lower and higher DhL concentrations, respectively. Clonogenic assays in the presence of DhL revealed that proliferating cells were very effectively eliminated by DhL due to the induction of apoptotic and senescence programs. Further analysis of the novel role of DhL in cellular senescence showed that the anti-proliferative effect was associated with a delay in progression through the G2 phase that preceded cell cycle arrest in the

following G1 phase. This phenomenon was accompanied by reduced cyclin B1 and higher p53 levels, suggesting that p53 might be responsible for promoting cell cycle withdrawal.

Cyclin B1 is the regulatory subunit of CDK1, which plays a pivotal role in the transition of the cell cycle from the G2 phase to mitosis [6]. The inhibitor of apoptosis protein (IAP) survivin, implicated in the inhibition of apoptosis, also promotes transition through the G2/M checkpoint of the cell cycle. Expression of this protein is controlled by a variety of mechanisms, including transcriptional mechanisms via β-catenin/Tcf-Lef, known to be highly relevant in many cancer types [7]. In melanomas, the loss or inactivation of cell death control contributes to resistance to chemotherapeutic drugs. This desensitization process involves a combination of strategies, including activation or upregulation of anti-apoptotic survival proteins (e.g. survivin) and inactivation of pro-apoptotic effectors. In many tumor cells, aberrant expression of cell cycle regulatory proteins (cyclins, CDKs, p21) also contributes to uncontrolled cell cycle progression [8].

In this study, we sought to obtain *in vivo* evidence for the efficacy of DhL in the treatment specifically of melanomas. To that end, we evaluated in a pre-clinical murine melanoma model whether DhL reduced the proliferation and growth of B16F0-derived melanomas in syngenic C57/BL6 mice. Our results confirmed that DhL was also anti-proliferative *in vitro* in B16F0 mouse melanoma cells. This phenomenon was accompanied by upregulation of p21, reduced cyclin D1, cyclin B1 and survivin levels, as well as reduced β-catenin/Tcf-Lef dependent transcription. Also, DhL induced either premature senescence or apoptosis in these cells depending on the concentration used.

Collectively, our findings indicate that DhL treatments lead to a significant reduction in the volume of tumors formed by B16F0 melanoma cells and do so by promoting senescence and apoptosis. Moreover, we determined using mathematical modeling that treatments with DhL for extended periods of time following preventive and therapeutic protocols were more effective than simultaneous treatments in reducing tumor volume.

Material and methods

Reagents

Dehydroleucodine (DhL) (structure: Fig. 1) at 93% purity, obtained as described in our previous study [5], was used from a stock solution of 0.4 M in DMSO. Peroxidase-labeled streptavidin was from Dako Denmark S/A (Glostrup, Denmark). Antibodies against cyclin B1, p21, p53 and survivin were from Santa Cruz Biotechnology (Santa Cruz, CA, USA). Antibodies against beta-actin were from Sigma-Aldrich (St. Louis, MO, USA).
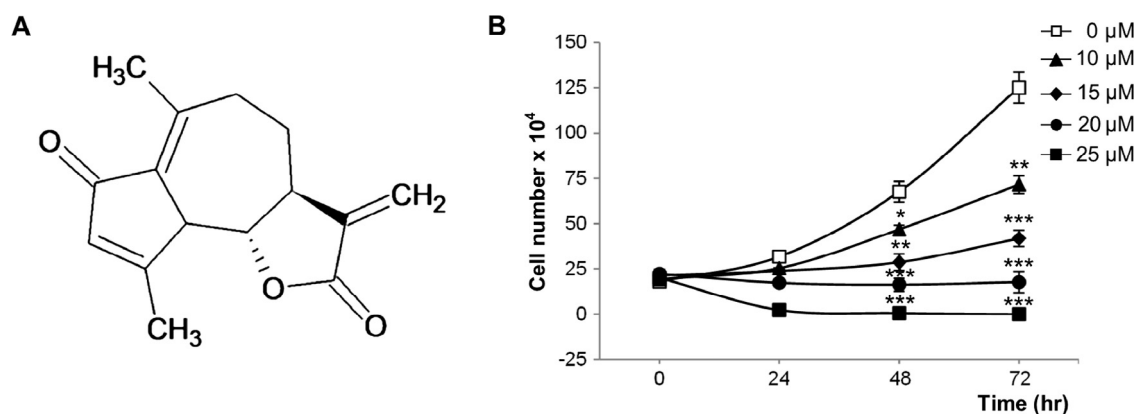
Animals

The animals used were 8–12-week-old C57BL/6 mice, born and housed in our animal facility, with a 12L:12D cycle and food and water *ad libitum* until they were sacrificed following CO_2 intoxication. Animals were maintained in accordance with the National Institutes of Health Guide for the Care and Use of Laboratory Animals. In each experiment, 8 male and 8 female mice from different cages were combined respectively. All procedures were approved by the Animal Research Committee of the Universidad Nacional de Cuyo (CICUAL). Authorization # 0028741/2010.

Cell lines and treatments

Murine melanoma B16F0 cells provided by Drs I. Hart, G. Moore and P. Parsons, were grown in RPMI1640 medium with 10% fetal bovine serum (FBS), 50 U/ml penicillin, and 50 µg/ml streptomycin in a humidified incubator with 5% CO2 at 37 °C. The cells were harvested after reaching 70–80% confluence and were plated either for subsequent passages or treatments with DhL. 2×10^5 cells were seeded in 6-well plates in RPMI1640 medium with 10% FBS for 12 h. Then the existing medium was replaced by fresh medium (RPMI1640, 10% FBS) containing DMSO or DhL (defined as time 0) and cultured for the specified periods of time. DMSO was used as a vehicle control in all experiments.

Cell proliferation assays

2×10^5 cells were treated with 0–25 µM of DhL for 72 h. To determine cell numbers, cells were trypsinized, suspended in regular medium, and counted with a Neubauer chamber.

Tumor growth assays

3×10^5 B16F0 cells in 200 µl PBS were injected subcutaneously into the right flank of C57BL/6 mice. After the indicated periods, 20 mg DhL in 20 µl DMSO/Kg/day or an equivalent volume of DMSO were injected daily into the right flank following three different protocols (preventive, simultaneous and therapeutic). In the preventive protocol, DhL or DMSO was injected 15 days prior to injection of B16 F0 cells. Alternatively, in the simultaneous protocol, DhL or DMSO was injected the same day as B16F0 cells, while in the therapeutic protocol DhL or DMSO was injected 8 days after the B16F0 cells. In each experiment, groups of 8 animals were used per treatment. The appearance of tumors was monitored by palpation. The tumor length and width were measured with a caliper and tumor volume was calculated using the following equation: volume = width$^2 \times$ length $\times \pi/6$ [9]. According to established bioethical regulations, tumors were measured until they reached a maximum of 2500 mm^3, at which point the animals were euthanized.

Towards the end of treatments, animals were sacrificed, and tumors were excised and prepared for histological analysis. For paraffin sections, tumors were fixed in 0.1 M phosphate buffer (pH 7.3)/formaldehyde 10% v/v for 48 h, dehydrated in alcohol, clarified in xylene, embedded in paraffin, and microtome sectioned at 5 µm. Paraffin-embedded histological slices were stained with hematoxylin-eosin (HE) for histological analysis.

Apoptosis assays

In vitro experiments: To determine early stage apoptosis, cells were stained with Annexin V using the Annexin V-FITC fluorescence detection kit (BD Biosciences San Jose, CA, USA) according to the manufacturer's instructions as described [5]. Briefly,

Fig. 1. DhL treatment inhibits cell proliferation in a dose-dependent manner.
The chemical structure of dehydroleucodine (left). B16F0 cells were treated with 0, 10, 20, or 25 µM DhL for 72 h and counted every 24 h (right). Data are expressed as the mean ± SEM of three independent experiments. * $p \leq 0.05$, ** $p \leq 0.01$, *** $p \leq 0.001$ vs. control group (0 µM DhL).

cells cultured on coverslips were treated with various concentrations (0–25 µM) of DhL for 24 h or 48 h, washed twice with PBS and then once with Annexin V Binding Buffer. The cells were stained with Annexin V-FITC diluted 1:10 in Annexin V Binding Buffer for 15 min at RT and fixed with 2% paraformaldehyde. The slides were examined and photographed with a Nikon Eclipse TE 2000 U motorized inverted microscope (Nikon Corp., Tokyo, Japan). The apoptotic index was calculated as the percentage of cells stained positive for Annexin V. Groups of 100 cells were counted in each experiment. Results from three independent experiments were averaged and values for apoptotic cells were expressed as the mean (%) ± SEM. In tumors: Apoptosis was assayed by the TUNEL assay in histological slices using the ApopTag Plus *in situ* detection kit (Oncor, Gaithersburg, MD, USA). Endogenous peroxidase activity was quenched by treatment with 3% H_2O_2 in PBS for 5 min. The coverslips were treated with 0.01 M citrate buffer (pH 3) heated to boiling temperature in a microwave oven for 30 min. Nucleotides were labeled according to the manufacturer's instructions. The coverslips were blocked with 10% bovine serum albumin (30 min at 20 °C), incubated overnight with biotin-conjugated mouse monoclonal anti-digoxigenin antibody at 4 °C, washed, incubated with biotinylated anti-mouse antibody for 45 min at room temperature, washed again, incubated with peroxidase-labeled streptavidin for 45 min at room temperature, washed briefly with PBS, and incubated with 0.5 mg/ml 3,3′ diaminobenzidine tetrahydrochloride/H_2O_2 for 10 min. The slides were counterstained with hematoxylin to reveal nuclei, then examined and photographed with a Nikon Eclipse E200 microscope (Nikon Corp., Tokyo, Japan). The apoptotic index was calculated as the percentage of positive nuclei based on an average of 400 cells in viable areas of 60 tumor histological slices in each experimental condition. Values for apoptotic cells from three independent experiments were averaged and expressed as the mean (%) ± SEM.

Senescence-associated β-galactosidase assays

In vitro experiments: *In situ* senescence-associated β-galactosidase (SA-β-Gal) staining was performed as described by Dimri et al. [10]. Briefly, cells were fixed with 2% formaldehyde and 0.2% glutaraldehyde for 5 min and incubated overnight at 37 °C with 1 mg/ml X-gal staining solution (5-bromo-4-chloro-3-indolyl β-D-galactoside, 5 mM K3Fe[CN]6, 5 mM K4Fe[CN]6, and 2 mM MgCl2 in PBS, pH 6.0). The cells were rinsed twice with PBS, washed with methanol and examined using a Nikon Eclipse E200 microscope (Nikon Corp., Tokyo, Japan).

In tumors: SA-β-Gal activity was monitored both in tumor cell extracts and *in situ* in cells of dissected tumors. Soluble SA-β-Gal levels in tumors cell extracts were determined as described by Lee et al. [11]. Briefly, tumor cell extracts were collected from tumors of DMSO or DhL mice, resuspended in extraction buffer and lysed by sonication. The samples were centrifuged at 13,000 × g for 1 h, and the resulting supernatants were mixed with 2.2 µg/µl 1,4-methyl-umbelliferon-β-D galactopyranoside (Sigma-Aldrich) in 1 mM MgCl2 phosphate buffer, pH 6 and incubated at 37 °C for 2 h. The reaction was terminated by adding two volumes of 1 M sodium carbonate. SA-β-Gal activity was monitored by measuring fluorescence emission at 360-448 nm with an Aminco Bowmen II Spectrophotofluorometer (American Instrument Co., Silver Spring, MD, USA). For this determination, equal amounts of tumor extracts prepared from DMSO or DhL treated mice were used. The activity of SA-β-Gal was expressed as picoM/weight of tumor.

Cells from dissected tumors were attached to coverslips, fixed in 2% formaldehyde and 0.2% glutaraldehyde for 5 min and incubated overnight at 37 °C with 1 mg/ml X-gal staining solution in PBS, pH 6.0. The coverslips were rinsed twice with PBS, washed with methanol and examined using a Nikon Eclipse E200 microscope. The number of cells positive for SA-β-Gal activity was assessed in a total of 300 cells on 5 coverslips from three experiments.

Gel electrophoresis and western blot analysis

Treated cells were washed twice with ice-cold PBS, pelleted and lysed by freeze/thawing in extraction buffer (50 mM HEPES, pH 7.5, 1 mM EDTA, 150 mM NaCl, 10 mM β-glycerophosphate, 1 mM NaF, 0.1% Triton X-100, 10% glycerol, with protease inhibitors) for 30 min on ice. The samples were centrifuged at 12,000 × g for 20 min at 4 °C and supernatants were collected. Protein concentrations were determined by the Bradford method [12]. Cell extracts were separated by SDS-PAGE and transferred to nitrocellulose membranes (BioRad Laboratories, Hercules, CA, USA). The membranes were incubated with antibodies against cyclin B1, p21, p53, survivin and β-actin for 2 h at room temperature and subsequently with the appropriate horseradish peroxidase-conjugated secondary antibodies. A SuperSignal West Pico chemiluminescent substrate kit (Pierce/ThermoFisher Scientific Inc., Rockford, IL, USA) was used to visualize protein bands that were quantified by scanning densitometry using the Image J program.

Plasmids

The luciferase reporter plasmids pTOP-FLASH (containing a promoter with three wild-type Tcf/Lef-binding elements/TBEs) and pFOP-FLASH (containing mutated TBEs) were provided by Dr. Hans Clevers (Hubrecht Laboratory, Uppsala, The Netherlands). The survivin reporter plasmids pLuc-1710 (containing a promoter with three TBEs) and pLuc420-M (containing a mutation of the crucial TBE) were kindly provided by Dr. DC Altieri [13].

Luciferase reporter assays

Tcf/Lef and 1710/3M reporter assays were performed as described [14]. Briefly, B16F0 cells were transfected with 2 µg of each plasmid: pTOP-FLASH (Tcf/Lef reporter), pFOP-FLASH (mutated Tcf/Lef binding site), pLuc-1710 (survivin promoter), pLuc420-3M (mutated promoter). After transfection (24 h) with individual plasmids, cells were lysed in a buffer containing 0.1 M KH_2PO_4 (pH 7.9), 1 mM DTT, 0.5% Triton X-100, centrifuged at 13,000 × g and supernatants (50 µl) were used to measure luciferase activity (serial dilutions in a 96-well plates). Luciferase activity was detected using a luminescence counter (Topcount, Perkin Elmer-Cetus, Boston, MA) after addition of KTME buffer containing 100 mM Tris-HCl, 10 mM $MgSO_4$, 2 mM EDTA, 5 mM Na_2ATP, and 0.1 mM luciferin. Luciferin activity data were standardized for each condition by calculating the TOP/FOP, pLuc-1710/pLuc420-3M activity ratios, respectively. Values shown are the mean ± SEM of activity measurements averaged from a least three independent experiments, where 100% was assigned to values obtained in control cells.

Mathematical model of implanted melanoma growth

To evaluate melanoma growth, a mathematical model based on the Gompertz law [15] was employed to fit experimental tumor volume registered in preventive, simultaneous and therapeutic protocols. The equation developed by Cabrales et al. [16], used with some modifications in equation (1), simulates tumor volume ($V_{(t)}$) at variable time points (t) of treatment. The equation (1) considers the tumor volume at time 0 of treatment (V_0) and two real and positive parameters, β and α that can be derived from the experimental data obtained using each protocol.

$$V_{(t)} = V_0 e^{\left(\frac{\beta}{\alpha}\left(1 - e^{(1-\alpha t)}\right)\right)} \tag{1}$$

V_0 was obtained from the average of initial tumor volumes of three experiments for each treatment; β represents the initial intrinsic growth rate of the tumor and α is the initial intrinsic growth of the tumor plus the modified tumor growth rate due to treatment. Both β and α were obtained using the method of least squares of experimental data. Data obtained for 7–11 days of treatment were fit to the equation (1) using the Wolfram Alpha Computational knowledge engine (Wolfram Research Company, Champaign, IL, USA).

Statistical analysis

The data shown are mean ± SEM from 3 independent experiments. Statistical analysis was performed using one-way ANOVA or paired two-tailed. Student's t-test (Prism 5 program, GraphPad Software Inc., La Jolla, CA, USA).

Results

DhL Inhibits proliferation of B16F0 mouse melanoma cells

Initially, B16F0 cells were treated with various concentrations of DhL for 72 h and the effects on cell growth were evaluated by counting cells. Cell number decreased by 40% with 10 µM DhL, 70% with 15 µM DhL, and almost by 100% with 20 µM DhL. Also, 25 µM DhL induced cell detachment after 24 h of treatment. The half maximal inhibitory concentration (IC50) for DhL after 72 h in culture was 12.5 µM (Fig. 1). These findings indicate that DhL reduces, in a dose dependent manner, B16F0 cell proliferation.

DhL upregulates p21 and downregulates the cyclins B1 and D1, as well as survivin

The permanent cell cycle arrest of B16F0 cells observed following treatment with 20 µM DhL suggested that cell cycle regulators were likely to be altered by DhL. Accordingly, we observed increased p21 levels after 24 and 48 h of treatment (Fig. 2), although the levels of p53 were not altered. Alternatively, cyclin D1, cyclin B1 and survivin levels decreased significantly after 24 and 48 h of treatment.

The β-catenin-TCF/LEF pathway is involved in transcription of many genes implicated in tumor development and progression, including survivin and cyclin D1. Based on this and given that DhL reduced cyclin D1 and survivin protein levels, we asked whether these effects of DhL may be attributed to changes in transcriptional activity of the β-catenin-Tcf/Lef. As anticipated, the treatment
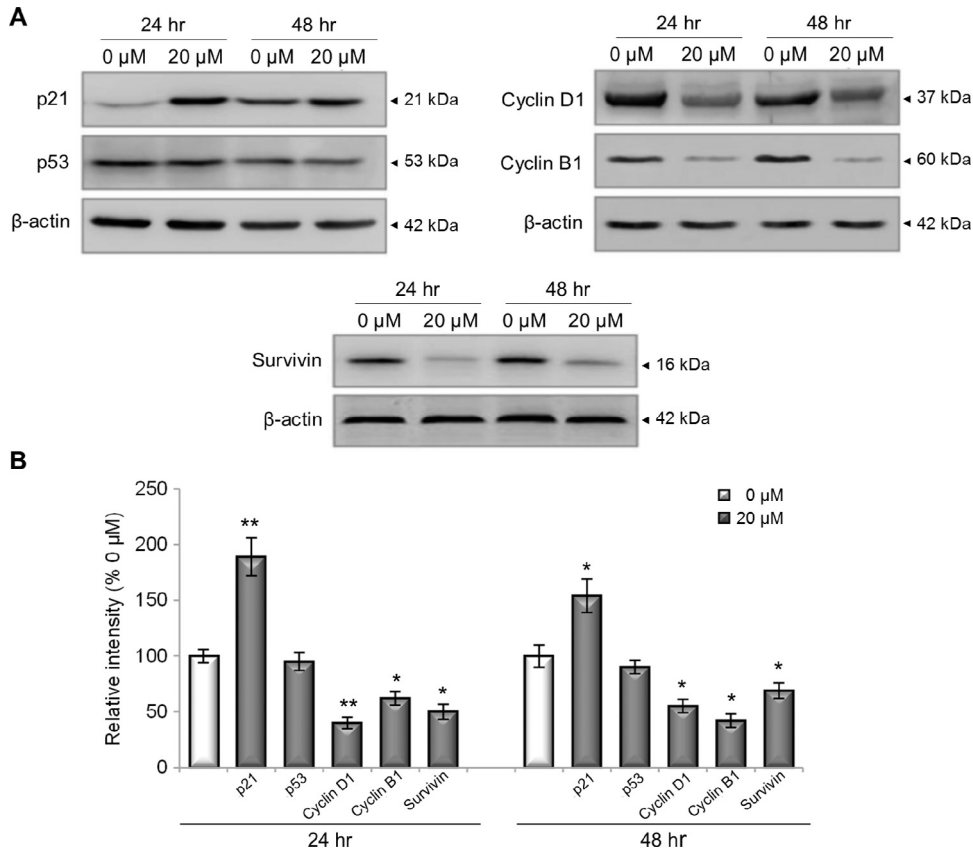
Fig. 2. DhL alters the expression of cell cycle proteins.
B16F0 cells treated with 0 (0 μM) or 20 μM (20 μM) of DhL were lysed at the indicated time points. (A) Immunoblot analysis of the proteins p21, p53, Cyclin D1, Cyclin B1 and survivin. The immunoblots shown are representative of three independent experiments with similar results. (B) Densitometric analysis of p21, p53, Cyclin D1, Cyclin B1 and Survivin normalized to β-actin. Band intensities are expressed as percentiles relative to the control (defined as 100%). Data shown are the mean ± SEM of values averaged from three independent experiments, * $p \leq 0.05$, ** $p \leq 0.01$ *** $p \leq 0.001$ for the treated group (20 μM) vs. control group (0 μM).

with 20 μM DhL for 24 h decreased the activity both of a generic TCF/LEF (40%) and the survivin-specific (50%) reporters (Fig. 3). These results suggest that DhL probably reduced the expression of cyclin D1 and survivin by inhibiting the β-catenin/TCF-Lef pathway (Fig. 3 left) and, importantly, DhL also reduced the activity of the survivin specific reporter (Fig. 3 right).

DhL triggered premature B16F0 senescence and apoptosis in a concentration-dependent manner

The reduction in cell number and the alterations in cell cycle proteins upon DhL addition (Figs. 1–3) may reflect the consequences of cell cycle arrest, cell death or both.
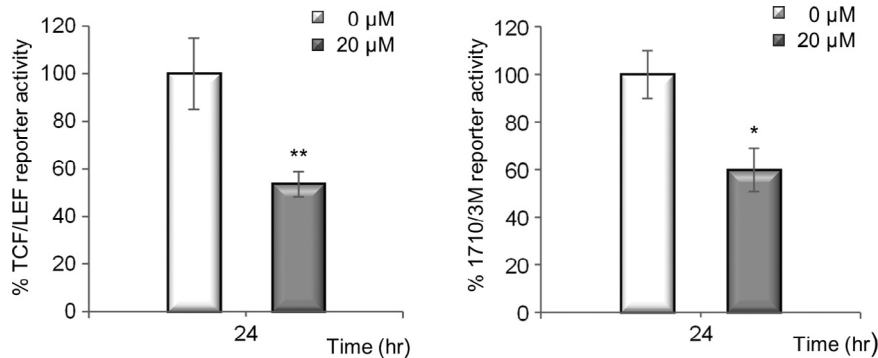

Fig. 3. DhL decreases the transcriptional activity of both β-catenin/Tcf-Lef and survivin promoter reporters. B16F0 cells were transfected with TOP/FOP flash or 1710/3M reporter constructs using lipofectamine. After 6 h of transfection, cells were treated with 0 (0 μM) or 20 μM (20 μM) DhL for 24 h. The cells were collected and centrifuged. Cell pellets were lysed and supernants were assayed for luciferase activity. Data shown are the mean ± SEM of values averaged from three independent experiments for TOP/FOP (left) and 1710/3M (right) reporters, respectively. * $p \leq 0.05$, ** $p \leq 0.01$ for the treated group (20 μM) vs. control group (0 μM).
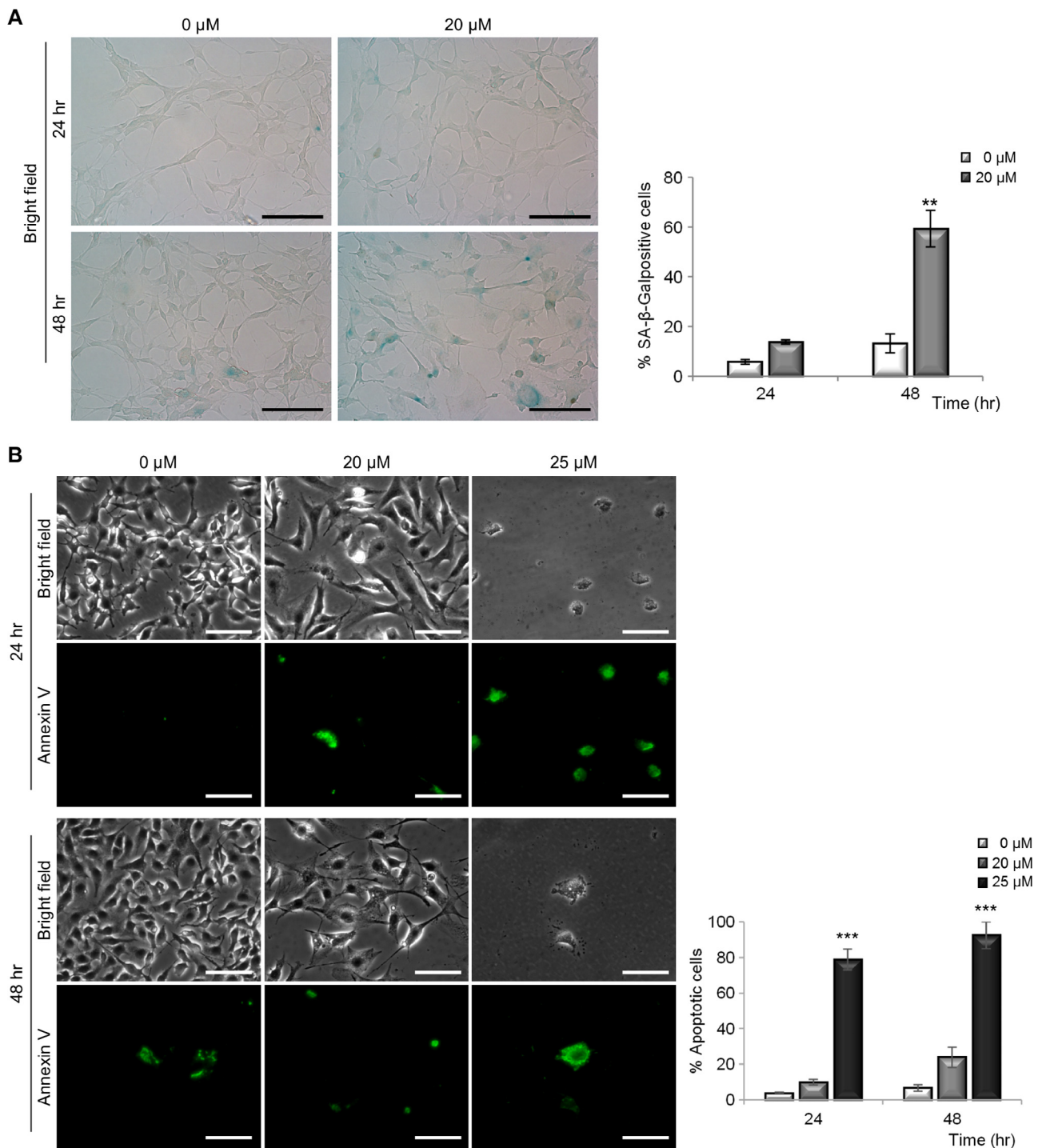
Fig. 4. DhL induces premature senescence and apoptosis *in vitro*.
B16F0 cells were treated with 0 (0 μM) or 20 μM DhL (20 μM) for 24 or 48 h. (A) Cellular senescence were assessed by evaluating SA-β-Gal activity at pH 6 *in situ*. Representative panels are shown for control and treated cells stained *in situ* for SA-β-Gal and examined by bright field microscopy (left). Bar: 50 μm. Percentages of SA-β-Gal-positive cells (Right).
(B) Apoptotic cells assessed by the Annexin V assay. Representative panels are shown with apoptotic cells indicated by arrowheads. Bar: 50 μm (left). Percentages of apoptotic cells after 24 and 48 h (right). Data shown are the mean ± SEM of values averaged from three independent experiments. * p ≤ 0.05, ** p ≤ 0.01, *** p ≤ 0.001 vs. control group (0 μM DhL).

Permanent arrest mediated by p21 has been linked in most cases to premature senescence [17], while reduced levels of survivin are associated with apoptosis [18]. Based on our previous observations in HeLa and MCF-7 cancer cells, we hypothesized that DhL may also promote senescence in B16F0 cells. We observed that cells treated with 20 μM DhL for 48 h were larger and flatter than control cells, and a striking increase in the number of cells that stained positive for SA-β-Gal activity *in situ* (nearly 60%) was observed (Fig. 4A).

Because 25 μM DhL reduced cell proliferation, the number of cells attached to the well (Fig. 1) and the expression of survivin (Fig. 2, 3), we analyzed whether DhL also induced cell death by apoptosis. The Annexin V assay for apoptosis showed that the treatment

with 20 μM DhL for 24 and 48 h did not increase the number of apoptotic cells, while following treatment with 25 μM DhL for 24 h, 80% of the cells were apoptotic (Fig. 4 B). Using Annexin V/Propidium Iodide double staining assay, we observed that 25 μM DhL generated substantial apoptosis without inducing a significant number of necrotic cells (Fig. S1). Notably, 25 μM DhL increased significantly caspase-3 activity (Fig. S2), confirming that treatment with 25 μM DhL triggered apoptosis.

DhL decreases the growth of melanomas implanted in C57/BL6 mice

Based on the previous findings, we evaluated the effect of DhL on the growth of experimental B16F0 melanomas in C57/BL6 mice. The dosage of DhL for *in vivo* treatments determined by toxicity analysis showed that doses up to 100 mg DhL/Kg/day/kg administered orally to mice did not have toxic effects (Guardia T, Universidad Nacional de San Luis, Argentina, personal communication). Moreover, doses up 20 mg DhL/Kg/day/kg injected subcutaneously into the right flank of mice did not produce skin lesions and thus this dose was used for the *in vivo* experiments. Effects of DhL were evaluated following three different protocols, referred to as preventive, simultaneous and therapeutic. To simplify nomenclature, mice treated with vehicle are referred to as control mice, while mice treated with DhL are DhL mice. In preventive protocols, at day 7 post-implantation, tumor volumes of control mice were about 370 mm^3 and reached volumes of 1000 mm^3 after 11 days. For DhL mice, tumor volumes were slightly smaller than in control mice (160 mm^3) at day 7 of treatment and significantly smaller at day 8 of treatment, reaching volumes of 170 mm^3 at day 11, indicating that DhL reduced the tumor volumes by 70% (Fig. 5A).

Following the simultaneous protocol, control mice had tumor volumes of 250 mm^3 at day 7 and 2500 mm^3 at day 14 of treatment (Fig. 5B). Alternatively, tumor volumes of DhL mice were 100 mm^3 at the day 7 and 1000 mm^3 at day 14 of treatment, indicating that DhL reduced tumor volumes by 60% following this protocol.

In therapeutic protocols, tumor volumes following treatment with vehicle in control mice were 250 mm^3 at day 7 and 2000 mm^3 at day 14 (Fig. 5C). In DhL mice, tumor volumes were 250 mm^3 at day 7 and 1000 mm^3 at day 14 of treatment, indicating that DhL treatment reduced tumor volume by 50% following this protocol.

After sacrificing the animals at the last day of the respective assays, the weights of tumors from DhL mice were reduced by 60% following the preventive protocol, by 80% following the simultaneous protocol and 40% following the therapeutic protocol (Fig. 5A, 5B, 5C, right). Note that the reductions in tumor mass recorded at the end of experiment day 14 following DhL treatment were similar for the different protocols (Fig. 5 A–C, left). Of note, the treatments with DhL neither affected the weight or overall survival of mice (data not shown).

DhL treatment alters the cell characteristics of implanted melanomas

In histological slices of melanomas, areas with viable cells growing in layers around blood vessels were observed. Beneath several layers of viable cells, a zone with necrotic cells was detected (Fig. 6A). On the last day of treatment with DhL, the necrotic area of tumors did not change significantly following preventive, simultaneous or therapeutic protocols (Fig. 6B). Nevertheless, for viable cells in tumors, nuclei were smaller and the cytoplasm was reduced (Fig. 7A). In simultaneous protocols, 40% of tumor cells in control mice displayed altered morphology, while in DhL mice this was the case for 80% of the tumor cells (Fig. 7A and B). Also, a higher percentile of altered cells was detected in areas of tumors with viable cells in DhL mice treated following simultaneous and therapeutic protocols (Fig. 7B).

In the tumors, areas with viable cells were detected in control mice (60 mitotic cells/mm^2) following the preventive protocol, while for tumors of DhL mice this number was reduced to 12 mitotic cells/mm^2 (Fig. 7C). Following the simultaneous and therapeutic protocols, DhL also generated a significant decrease in mitotic cells (Fig. 7C). Thus, DhL reduced the number of mitotic cells in tumors following all three protocols.

DhL induces premature senescence and apoptosis in B16F0 melanomas

Based on the aforementioned results (Figs. 1–4), we asked whether DhL induced premature senescence and apoptosis in melanomas *in vivo*. The presence of premature senescence was analyzed in tumors by the detection of SA-β-Gal both in tumor supernatants and *in situ* in melanoma cells. For the simultaneous and therapeutic protocols, SA-β-Gal was of 40 picoM/g × 10^5 and 60 picoM/g × 10^5, respectively, in tumor supernatants of control mice, and for DhL mice SA-β-Gal activity was 80 picoM/g × 10^5 and 100 picoM/g × 10^5, respectively (Fig. 8A), indicating that DhL increased by 65% SA-β-Gal activity following both protocols. Also, the number of cells from dissected tumors that were positive for SA-β-Gal activity *in situ* increased (Fig. 8B). Following the simultaneous and therapeutic protocols, 5% and 8% of cells, respectively, were senescent in tumors of control mice, while in tumors of DhL mice, these values increased to 25 and 30%, respectively (Fig. 8C).

The presence of apoptotic cells was detected in the viable area of histological slices of tumors using the TUNEL assay (Fig. 9A). Following the preventive protocol, 5% of apoptotic cells were detected in tumors of control mice, while this value increased to 30% in tumors of DhL mice (Fig. 9B). In tumors of mice treated following the simultaneous and therapeutic protocols, 5 and 7% of apoptotic cells were detected in tumors of control mice respectively, while these values increased to 20 and 30% of apoptotic cells, respectively, in tumors of DhL mice (Fig. 9B).

Taken together, these results indicate that DhL increased both the number of apoptotic and senescent cells in tumors of mice treated following all three protocols.

Early and late effects of DhL on the growth kinetics of melanomas

Model equations: The comparison of DhL effects on tumor growth kinetics following the three protocols used in this study is constrained by ethical considerations regarding animal well-being. We therefore simulated prolonged treatments using an equation that permitted mathematical modeling of melanoma growth (see equation 1 in Materials and Methods), to fit our experimental tumor volume data recorded up to the eleventh day after implantation. The following pairs of fitted equations were generated by least square regression analysis for control (1.1, 1.3, 1.5) and DhL treatment following preventive (1.2), simultaneous (1.4) and therapeutic (1.6) protocols.

$$V_{(t)} = 366.57e^{2.454\left(1-e^{(1-0.146t)}\right)} \tag{1.1}$$

$$V_{(t)} = 173.04e^{2.126\left(1-e^{(1-0.139t)}\right)} \tag{1.2}$$

$$V_{(t)} = 281.8e^{3.222\left(1-e^{(1-0.156t)}\right)} \tag{1.3}$$

$$V_{(t)} = 173.0e^{3.482\left(1-e^{(1-0.120t)}\right)} \tag{1.4}$$

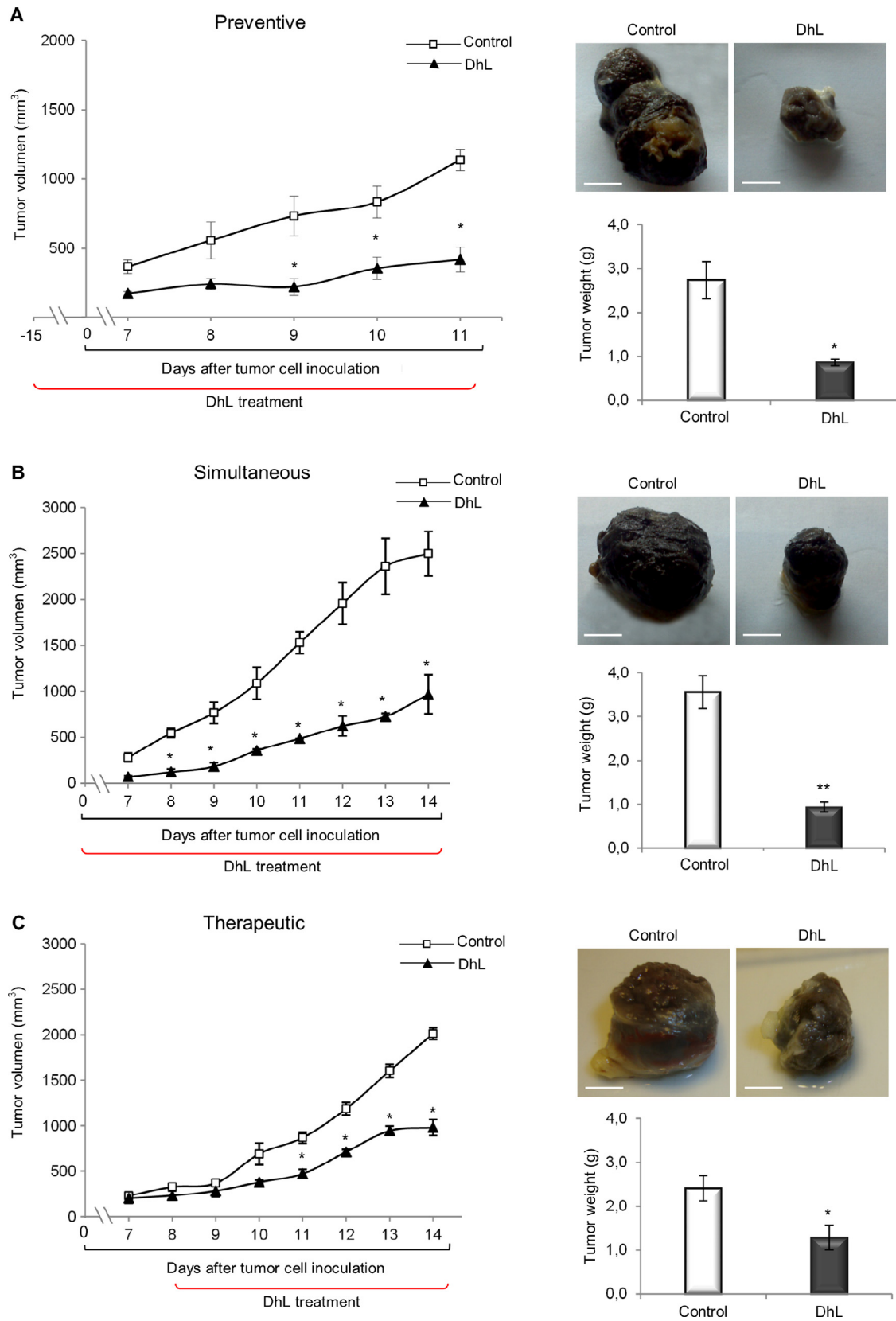$$V_{(t)} = 228.7e^{3.817\left(1-e^{(1-0.131t)}\right)} \tag{1.5}$$

Fig. 5. DhL slows the growth of murine melanomas. Time-course of tumor growth showing volume (left), tumor size (right upper) and tumor weight (right lower) on the last day of treatment for control (control) or DhL (DhL) mice, following preventive (A), simultaneous (B) and therapeutic (C) protocols. Data shown are the mean ± S.E.M. of values averaged from three independent experiments * p ≤ 0.05.

A

Preventive

Control   DhL
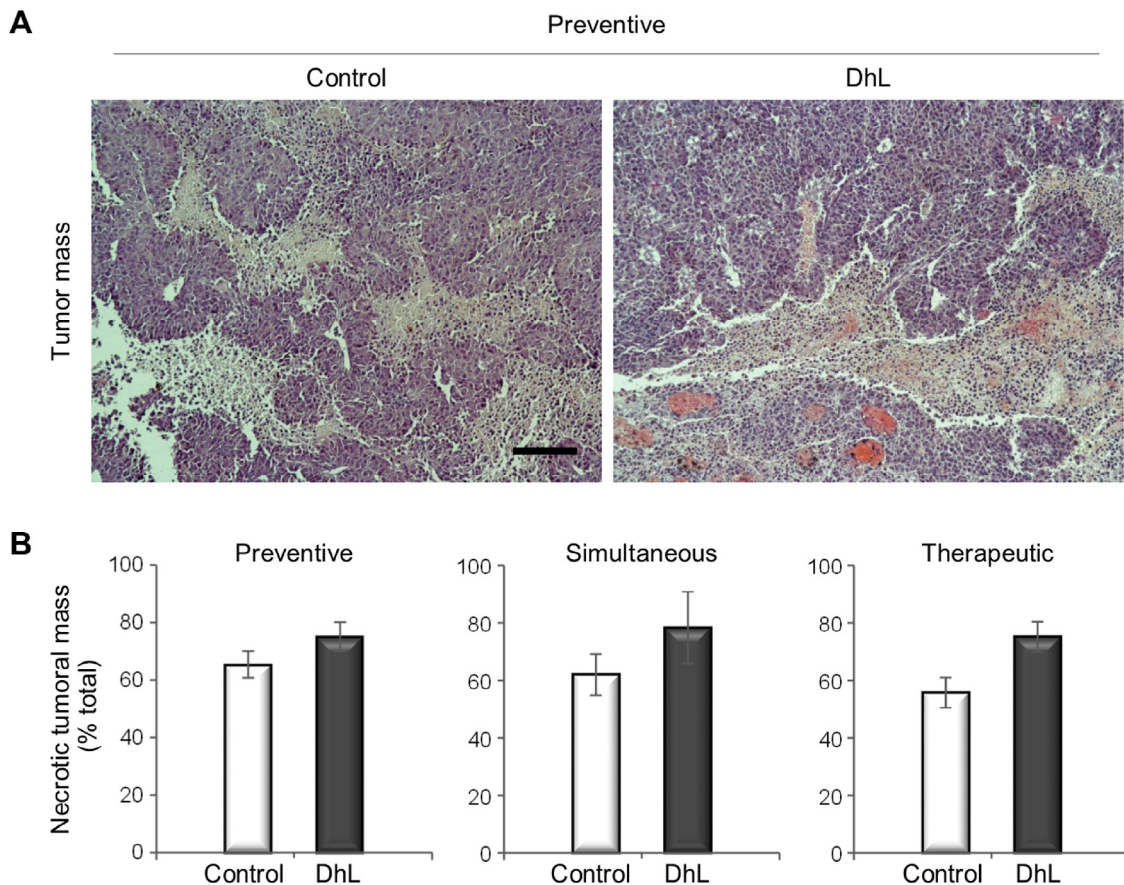
Tumor mass

B

Fig. 6. DhL did not increase the necrotic area of murine melanomas. (A) Paraffin-embedded histological sections of tumors obtained day 11 of treatment following the preventive protocol were stained with EH: control mice (left) and DhL mice (right). Bar: 50 μm. (B) Percent of necrotic tumor areas in paraffin-embedded histological sections of tumors from mice following the preventive (left), simultaneous (center) and therapeutic protocols after 11 days of treatment: results for control mice (control) and DhL mice (right) are shown. Data shown are the mean ± S.E.M. of values averaged from three independent experiments, p > 0.05.

$$V_{(t)} = 201.7e^{3.012\left(1-e^{(1-0.127t)}\right)} \qquad (1.6)$$

For tumors obtained following the preventive protocol, the equation-derived values of V_0, α and β were 366.57 mm³, 0.146 and 0.358 for tumors from control mice (equation 1.1), and 173.04 mm³, 0.139 and 0.296 for tumors from DhL mice (equation 1.2), respectively. Similarly the values for V_0, α and β were derived from the fitted equations for tumors obtained using the simultaneous (equations 1.3 and 1.4 for control and DhL mice, respectively) and the therapeutic protocols (equations 1.5 and 1.6 for control and DhL mice, respectively).

Curves generated by the model equations: Fig. 10A shows the data obtained in experiments after 0–11 days and the best-fit curves generated by least square regression for tumor volumes in control and DhL mice following the three protocols. In all cases, there was a close fit between the experimental data and model curve, with only a couple of outlying points in the simultaneous and therapeutic protocols. In Fig. 10B the derived equations were used to simulate longer DhL treatments. The resulting curves are all sigmoidal in shape with three sequential characteristics: an initial exponential growth phase is followed by an inflection point and then a phase of asymptotically decreasing growth. The 60 day projection following the preventive protocol (equation 1.1, 1.2) for control mouse data predicted a maximum tumor volume at day 40 of 4320 mm³, with the inflection point at day 13 when the tumor volume was expected to be 1560 mm³ and growth velocity (gv) was estimated at 228 mm³ /day. Nevertheless, the predicted tumor volume of DhL mice at day 40 reached values of only 1400 mm³, and importantly no further increase in volume up

to day 60 was expected. The inflection point was reached at day 12 with a tumor volume of 520 mm³ and an estimated gv of 73 mm³/day. In the simultaneous protocol (equation 1.3, 1.4), control mouse data predicted a maximum tumor volume at day 40 of 7000 mm³, with the inflection point at day 13, a tumor volume of 2600 mm³ and gv of 407 mm³/day. On the other hand, the tumor volume of DhL mice reached the maximum value of 5100 mm³ at day 50 with the inflection point at day 16, a tumor volume of 2070 mm³ and gv of 249 mm³/day. Following the therapeutic protocol (equation 1.5, 1.6), the tumor volume of control mice was predicted to reach 10,500 mm³ after 60 days and continue growing. The inflection point increased to day 18 at which point the tumor volume was expected to be 3800 mm³ and gv 503 mm³/day. On the other hand, the tumor volume in DhL mice reached a predicted maximum value of only 4000 mm³ at day 50, with the inflection point at day 16, a tumor volume of 1500 mm³ and gv of 192 mm³/day.

Considering the projected maximum tumor volume the last day of DhL treatment together with the tumor volume and gv reached at the inflection point, it becomes apparent that both the preventive and therapeutic protocols are more efficient than the simultaneous protocol in reducing predicted growth up to day 60 (Fig. 10B).

In order to evaluate the comparative efficacy of the DhL treatment protocols, we estimated the relative difference in tumor volume of DhL mice compared to the control mice. In the early part of the treatment (0–11 days), the simultaneous and preventive protocols were more efficient in reducing tumor volume than the therapeutic protocol (Fig. 10C, left panel). Nevertheless, after day
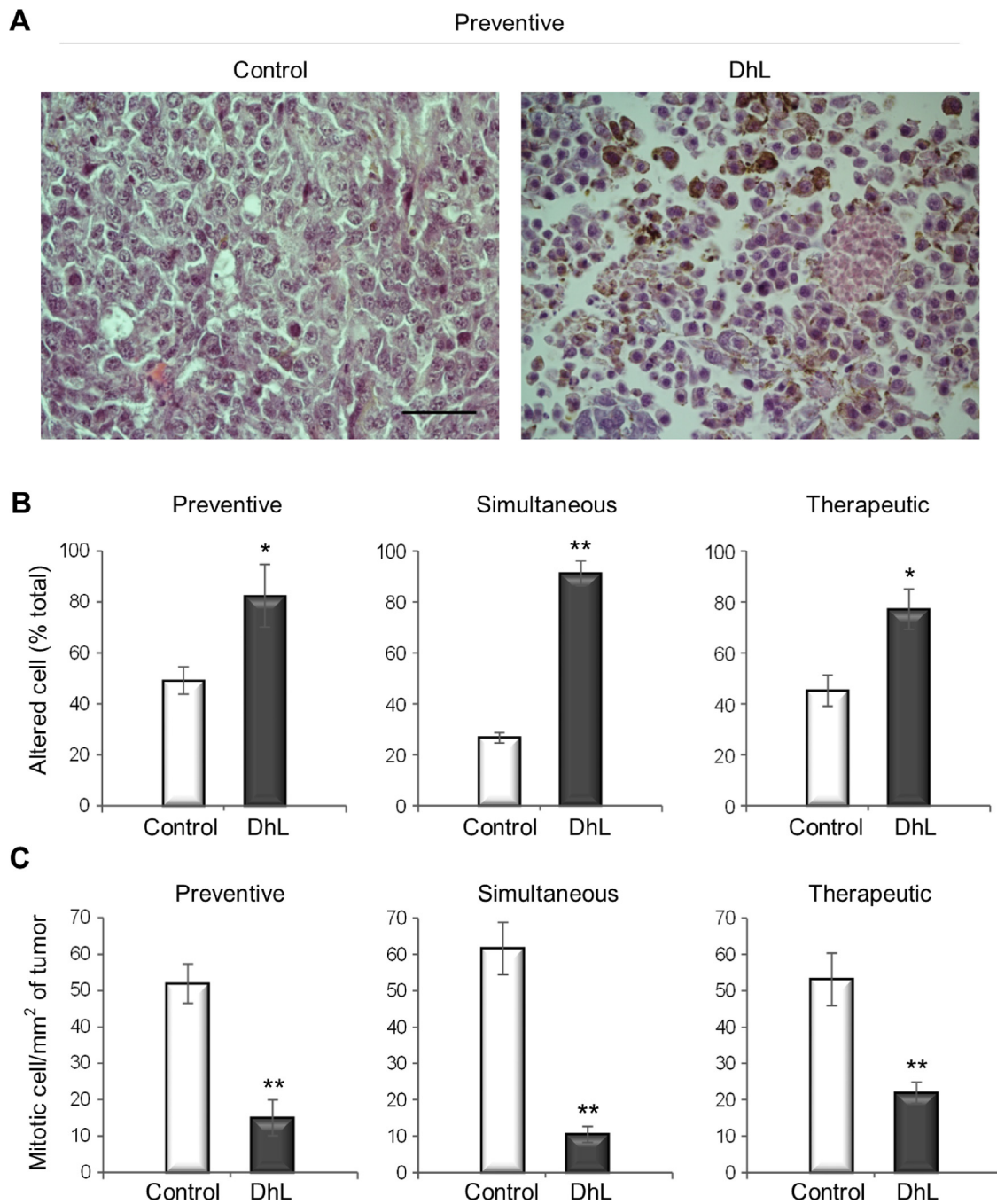
A

Preventive

Control   DhL

B

C

Fig. 7. DhL increased the number of altered cells and decreased the number of mitotic murine melanoma cells. (A) Paraffin-embedded histological sections stained with EH of tumors after 11 days following the preventive protocol: control mice (left) or DhL mice (right). Bar: 50 µm. (B) Percent of altered cells in paraffin-embedded histological sections in tumors from mice after either 11 days of treatment following the preventive protocol (left); 14 days following the simultaneous protocol (center) or 14 days following the therapeutic protocol (right): results for control mice (control) and DhL mice (DhL) are shown, *$p \leq 0.05$ and **$p \leq 0.01$. (C) Number of mitotic cells per square mm in paraffin-embedded histological tumor sections from mice after 11 days following the preventive protocol (left); 14 days following the simultaneous protocol (center) or 14 days following the therapeutic protocol (right): results for control mice (control) and DhL mice (DhL) are shown. Mitotic cells (metaphase, anaphase and telophase) were counted in 70 fields of 40 X (0.07 mm^2) of 5 histological sections for each experiment. Data shown are the mean ± S.E.M. of values averaged from three independent experiments, **$p \leq 0.01$.

20 of treatment the relative differences between the projected curves for DhL mice (Fig. 10B) suggested that the preventive and therapeutic protocols were likely to be more efficient in reducing tumor volume than the simultaneous protocol (Fig. 10C, right panel).

Discussion

Malignant melanoma represents one of the most lethal cancer types often attributable to early metastasis and failure of chemotherapy due to the development of resistance to anti-neoplastic drugs. To improve outcome, new drugs are required that target a variety of mechanisms in these cancer cell cells. Mouse melanoma cell lines are useful models for identifying key molecular events involved in disease progression, and providing potential preclinical models to evaluate the therapeutic potential of compounds [19]. Specifically, the availability of a pre-clinical tumorigenesis model involving subcutaneous growth of B16F0 melanoma cells in syngenic C57/BL6 mice allowed us to determine the efficiency of DhL in
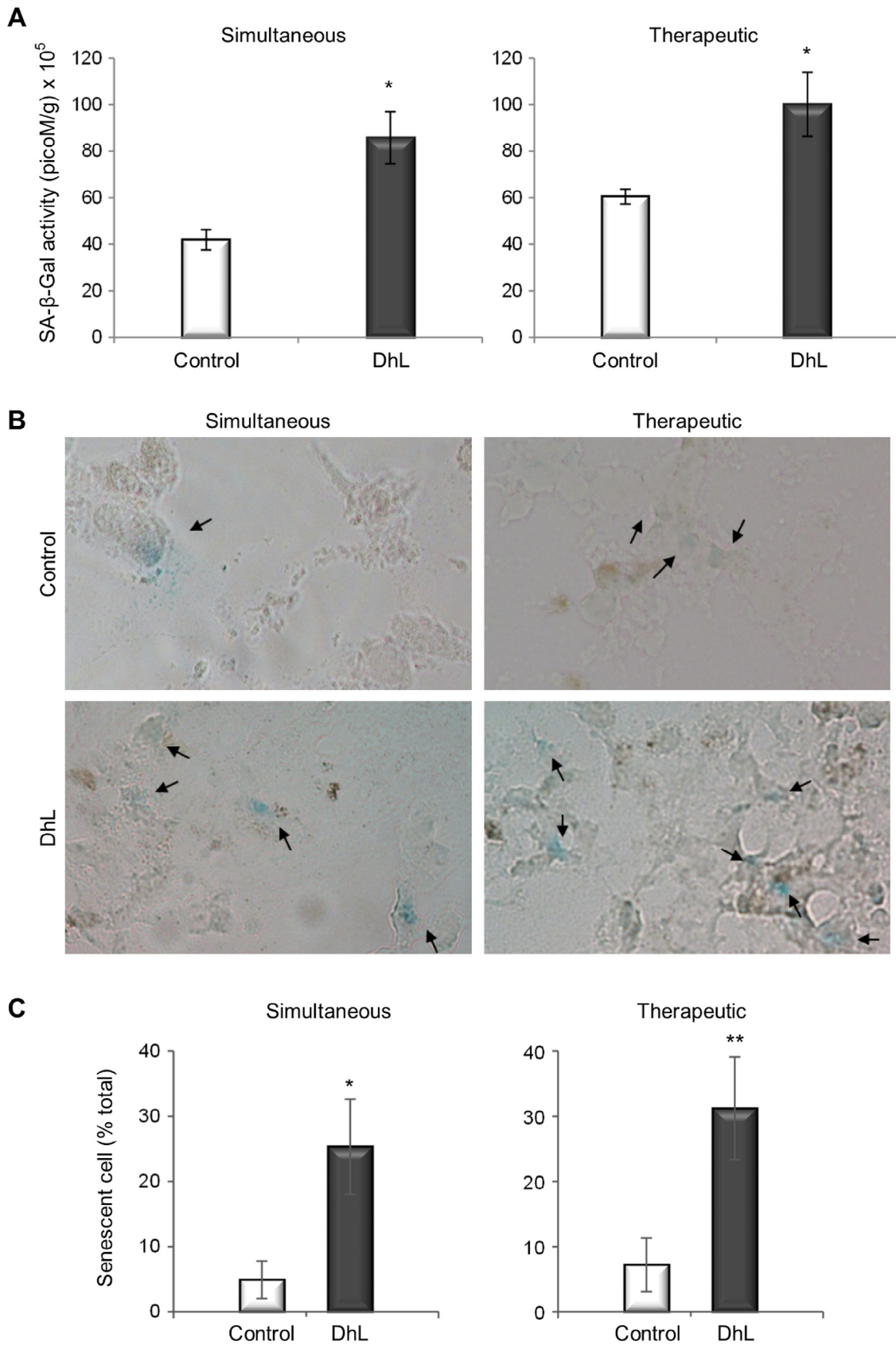
Fig. 8. DhL increased the number of senescent murine melanoma cells. (A) SA-β-Gal activity in cell extracts from tumors from mice following the simultaneous (left) and therapeutic protocols (right), *p ≤ 0.05. (B) SA-β-Gal activity in tumor sections from mice following the simultaneous (left) and therapeutic protocols (right). Arrows indicate SA-β-Gal positive cells. (C) Percent of senescent cells compared to the total number of cells (100%) in tumor sections from mice following the simultaneous (left) and therapeutic protocols (right). Data are the mean ± S.E.M. of values averaged from three independent experiments. *p ≤ 0.05 and **p ≤ 0.01.
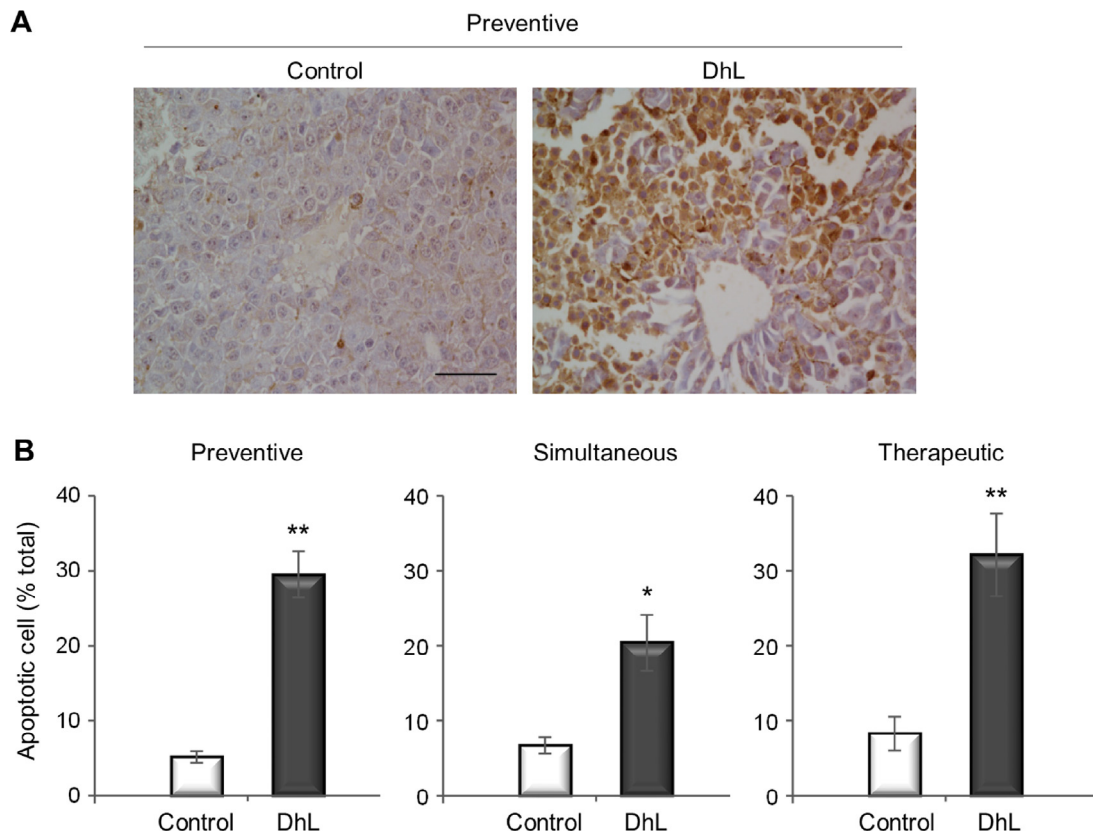
A

Preventive

Control | DhL

B

Fig. 9. DhL increased the number of apoptotic murine melanoma cells. (A) TUNEL assay in histological sections of tumors from mice treated 11 days following the preventive protocol: results are shown for control (left) and DhL mice (Dh) (right). Note that sections were post-stained with EH. Bar: 50 μm. (B) Percent of apoptotic cells detected by TUNEL assay. Apoptotic cells were counted in 70 fields at 40× magnification (0.07 mm^2) for three histological sections in three independent experiments. Data are the mean ± S.E.M. of values averaged from three independent experiments, $^*p \leq 0.05$ and $^{**}p \leq 0.01$.

suppressing tumor cell growth initially *in vitro* and then *in vivo*. In this study, we show using *in vitro* assays that DhL arrested B16F0 cell proliferation in a dose-dependent manner by causing apoptosis and senescence. Also, cell cycle control was affected by DhL. *In vivo*, our results show that DhL has potent anti-tumor effects in a pre-clinical melanoma model. Moreover, we obtained evidence indicating that tumor suppression is likely attributable to combined modulation of all these mechanisms, although they are probably induced at different *in situ* concentrations of the drug.

The mechanism of action of SLs remains poorly understood. The biological activities of these compounds have been attributed to various factors, including alkylating center reactivity, side chains, lipophilicity, and molecular or electrical features [2,20]. Thapsigargin, a SL compound that is currently being evaluated in phase I clinical trials, induces apoptosis via signals that involve inhibition of the sarco/endoplasmic reticulum calcium ATPase (SERCA) pump and the release of cytochrome c from mitochondria [20,21]. DhL is an SL that also belongs to the guaianolide group and has the same cyclic carbon skeleton as does thapsigargin; however, we found that the molecular pathways that are activated by DhL treatment are not restricted to the ER/mitochondria and cytoplasm. The accumulation of DNA damage response (DDR) markers in the nucleus may be a trigger for apoptotic and senescence programs. Indeed, the latter represent important anti-cancer mechanisms that we previously reported were associated with SL treatment of cancer cells [5]. The fact that DhL limited melanoma growth by promoting both senescence and apoptosis underscores the potency and selectivity of this SL as a novel, promising pharmacological agent with antitumor activity.

Results implicating p21 in preventing tumor growth are somewhat controversial. Indeed, loss of p21 contributes to increased

tumorigenic potential in both melanoma cell lines and human melanomas [8] and the introduction of p21 into mice expressing inactive p53^{R172P} generated tumor suppression by senescence [22,23]. Furthermore, introduction of this p53^{R172P} gen into p21 null mice results in complete loss of the cell cycle arrest response and enhanced tumorigenicity [24]. Taken together, these results suggest that activation of p21 is important for senescence-dependent tumor suppression. However, a recent study showed that although p21 plays an important role in mediating the p53-dependent cellular response to stress, lack of p21 does not necessarily promote tumor development [25]. Also, induction of senescence as a tumor suppressor mechanism is still controversial. Although a considerable body of experimental evidence favors the interpretation that senescence functions as a tumor suppressor mechanism [26], some studies suggest that senescent cells in the tumor stroma could promote proliferation and transformation of the underlying epithelium [27,28]. In any case, our results indicate that DhL induced senescence and apoptosis, as well as reduced proliferation of melanoma cells, and associated these observations with significant inhibition of tumor growth *in vivo*. Thus, in the context of our model, DhL-enhanced senescence (regulation of p21) is likely to be functioning as a tumor suppressor mechanism.

Together with senescence and apoptosis, we found that the treatment of B16F0 cells with DhL altered the expression of key proteins participating in tumor cell cycle progression. DhL decreased the levels of cyclin D1 and cyclin B1 (cell proliferation) but increased expression of the cell cycle arrest protein p21. Also, DhL decreased expression of the IAP survivin and reduced β-catenin-Tcf/Lef-dependent transcription. These observations provide strong molecular evidence for an additional role of DhL as an inhibitor of
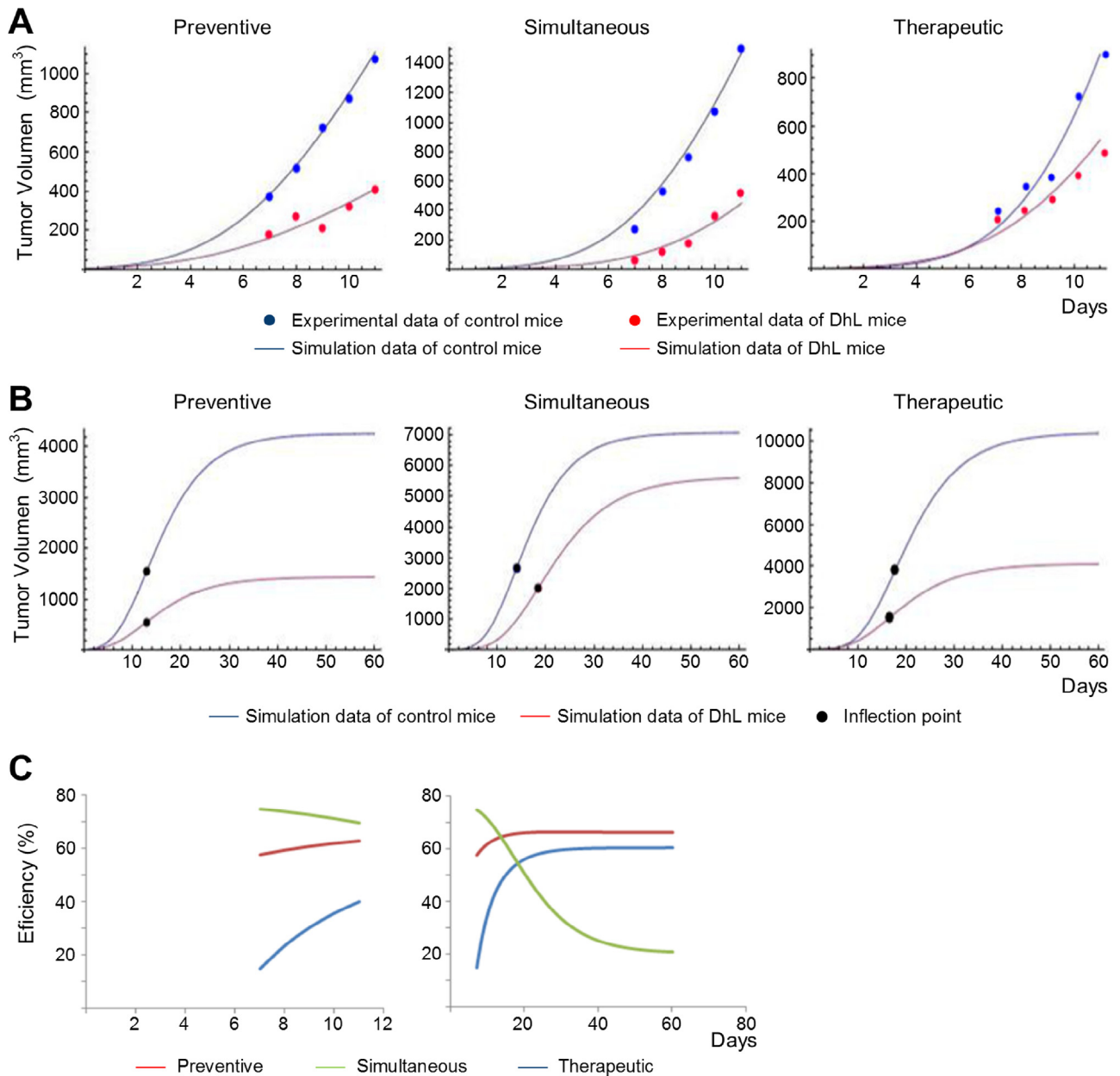
Fig. 10. Mathematical modeling of the effect of DhL on melanoma growth. (A) Growth curves obtained both by *in vivo* measurement and mathematical modeling of tumors in mice following preventive (left), simultaneous (center) or therapeutic (right) treatment protocols: results are shown for control (blue dots and blue line, respectively) and DhL mice (red dots and red line, respectively). (B) Predicted growth curves for melanomas in mice after 60 days following the preventive (left), simultaneous (center) or therapeutic (right) treatment protocols: results are shown for control (blue line) and DhL mice (red line). Inflection points are indicated with a black dot. (C). Efficiency of DhL in reducing tumor volume in DhL mice following the preventive (red), simultaneous (green) and therapeutic (blue) treatment protocols up to 11 days (left panel) or 60 days (right panel), respectively. Treatment efficiency was calculated as the percentile of the relative difference in tumor volume between DhL and control mice divided by tumor volume of control mice for each day of the experimental or simulated treatments.

cell cycle progression in B16F0 cells. Signaling events that favor progression of the cell cycle have been implicated in the development of tumors [29,30]. Several lines of evidence point to the over-expression and participation of cyclin D1 protein in breast cancer and melanoma formation and melanoma metastasis [31–33]. The activating V600E mutation of the B-RAF oncogene, present in approximately 50% of cutaneous melanomas [34], is responsible for the increased phosphorylation of extracellular receptor activated protein kinases (ERKs) and increased expression of cyclin D1, which is associated with progression through the G1/S phase of the cell cycle [35]. In Sk-Mel-28 melanoma cells, synergism between B-RAF mutation and the over-expression of cyclin D1 are held responsible for the high growth rates of these cells and their refractoriness to cell-cycle blocking drugs [36]. Also, the natural polyphenol Rottlerin reportedly reduces Sk-Mel-28 melanoma growth by downregulating Cyclin D1 [37], and altered expression of cyclin B1 has been reported in numerous cancers, where it may contribute to chromosomal instability [38]. Furthermore, several studies have demonstrated the clinical significance of cyclin B1 over-expression as a factor indicative of poor patient prognosis and radiotherapy resistance in several cancer types, including melanoma [39,40]. Bearing in mind these observations, it is likely that the effects of DhL on cell cycle progression reported here for B16F0 cells are attributable in part to changes in Cyclin D1 and Cyclin B1 expression.

In tumors, the overexpression of survivin is known to be associated with tumor progression, metastasis and angiogenesis [7]. Also, survivin is over-expressed in essentially all human cancers and generally absent in normal adult tissues [7,41]. Given the relevance of survivin in cancer, the fact that DhL reduced survivin protein levels and inhibited directly the activity of a generic reporter construct for β-catenin/Tcf-Lef-dependent transcription, as well as the activity of a construct containing the Tcf-Lef binding sites in the survivin promoter region (Fig. 3), indicate that DhL suppresses a key pathway implicated in tumor development [7], likely by downregulating survivin expression, a protein known to strongly favor tumor survival and progression.

Bioethical considerations generally limit the possibilities of studying long-term effects of drug administration. Indeed, evaluating therapeutic efficacy is very much limited by the rapid tumor growth observed in this pre-clinical melanoma model. Thus, melanoma growth in mice could only be directly evaluated for a very limited window of time. To gain insight as to how DhL may impact on tumor development over extended periods of time, a mathematical model was employed that simulates DhL effects beyond the experimental time frame and allows theoretical comparisons of the efficacy of the protocols used. Following this procedure, we found that during the first days of DhL treatment (days 0–11), preventive and simultaneous protocols were more effective in preventing growth tumor than therapeutic protocols. However, for longer treatments (up to 60 days), DhL was predicted to be most effective following preventive, followed by therapeutic and ultimately simultaneous protocols. This may be interpreted as indicating that early administration of DhL to mice stimulates intrinsic defense mechanisms that help reduce tumor growth. An intriguing possibility in this context is that preventive administration may lead to activation of the immune system and hence more effective systemic control of tumor cell growth.

In our studies, we observed that DhL downregulated β-catenin-Tcf/lef-dependent transcription in B16F0 cells. In addition to modulating the expression of survivin and many other cancer-related targets, this pathway has been implicated in modulating the host immune resistance to tumor growth. Specifically, it was recently demonstrated that melanoma-intrinsic β-catenin signaling reduces T-cell infiltration and prevents anti-tumor immunity in melanoma [42]. Analysis of the tumor microenvironment in patients with melanoma has revealed evidence of T-cell infiltration phenotype in many tumors [43,44] and the presence of activated CD8^{+}T cells both in tumors and the peri-tumoral stroma correlated favorably with patient prognosis [45,46]. Alternatively, depletion of T-cell-mediated immune responses results in rapid tumor growth in experimental animal models [47]. CD8^{+}T cells recognize the tumor-specific antigens, produce interferon-ɣ and induce cytostasis and cell death. Also CD8^{+}T cells promote cell cycle inhibition, apoptosis and angiostasis, and induce tumoricidial activity of macrophages in the tumor microenvironment [48,49]. Thus, in addition to the direct effects of DhL in melanoma cells demonstrated here, it also possible that stimulation of T-cell infiltration of melanomas may contribute to the effects observed *in vivo* [20,50]. Studies are currently in progress to evaluate this intriguing possibility in experimental melanomas.

In a previous study by our group, senescence and apoptosis in HeLa and other cell lines treated with DhL was associated with the amount of DNA breaks that were generated [5]. DhL treatment activated different DNA damage response pathways that, at low concentrations, induced cell cycle arrest by regulating cyclin/Cdk via checkpoint inhibitors and, at high concentrations, triggered cell apoptosis by a p53-dependent pathway [51,52]. Although it is tempting to speculate that this sharp concentration-dependent distinction between apoptosis and senescence observed in melanomas may be ascribed to similar mechanisms, further studies are required to resolve the underpinnings of this DhL-induced switch in melanomas. Nonetheless, bearing in mind that accessibility of drugs to different tissues may vary tremendously, the relevance of our findings at this point resides in revealing the capacity of DhL to prevent the proliferation of melanomas by a variety of mechanisms operating at different concentrations of the drug. Importantly, DhL decreased the number of cells in division, and increased significantly the number of senescent and apoptotic cells in tumors. Thus, DhL suppresses melanoma growth *in vivo* by a variety of tumor suppressor pathways that require different concentrations of the drug to be activated. In doing so, the window of therapeutic opportunity for DhL *in vivo* is greatly expanded.

Importantly, although several SLs inhibit *in vitro* proliferation of human melanoma cells: 1. Dehydrozaluzanin C and cynaropicrin [53], 2. Asteriscunolide A [54], 3. Parthenolide [55], 4. Several SL from Gonospermum gomerae and G. fruticosum [56]; 5. SL from Alphasantonin [57] and B16 mouse melanoma cells: 1. SL from Largehead Atractylodes Rhizome [58], 2. Vernolide-A [59]; only for two SLs have *in vivo* effects in melanomas been reported to date, namely for millerenolide and vernolide-A, which inhibit melanoma formation and metastasis, respectively [1,60,61]. However, neither of these studies provided insight to the mechanisms involved nor compared protocols evaluating how the drugs are most effectively administered to arrest primary site melanoma growth. Also, in the assays evaluating inhibition of metastasis by vernolide-A [61], it is difficult to infer that vernolide-A inhibited tumor growth because the size of lung tumor nodules was not reported. Assays are currently underway in our laboratory to determine whether DhL inhibits both melanoma growth and metastasis.

In summary, our results indicate that DhL has potent anti-tumor effects in a pre-clinical melanoma model that are attributable to a variety of mechanisms, including the ability to induce cell cycle arrest, as well as by triggering senescence and apoptosis. This broad spectrum of effects, and particularly the fact that these activities become apparent at different concentrations, makes DhL an extremely interesting target compound to consider for the future development of effective drugs for the treatment of melanomas and potentially other cancers.

Conflict of interest

The authors do not have any conflict of interest.

Appendix: Supplementary material

Supplementary data to this article can be found online at doi:10.1016/j.canlet.2015.12.004.

References

[1] P.G. Taylor, O.A. Dupuy Loo, J.A. Bonilla, R. Murillo, Anticancer activities of two sesquiterpene lactones, millerenolide and thieleanin isolated from Viguiera sylvatica and Decachaeta thieleana, Fitoterapia 79 (2008) 428–432.

[2] A. Ghantous, H. Gali-Muhtasib, H. Vuorela, N.A. Saliba, N. Darwiche, What made sesquiterpene lactones reach cancer clinical trials?, Drug Discov. Today 15 (2010) 668–678.

[3] H.A. Priestap, K.A. Abboud, A.E. Velandia, L.A. Lopez, M.A. Barbieri, Dehydroleucodin: a guaiane-type sesquiterpene lactone, Acta Crystallogr. Sect. E Struct. Rep. Online 67 (2011) o3470.

[4] O.S. Giordano, E. Guerreiro, M.J. Pestchanker, J. Guzman, D. Pastor, T. Guardia, The gastric cytoprotective effect of several sesquiterpene lactones, J. Nat. Prod. 53 (1990) 803–809.

[5] V.V. Costantino, S.F. Mansilla, J. Speroni, C. Amaya, D. Cuello-Carrion, D.R. Ciocca, et al., The sesquiterpene lactone dehydroleucodine triggers senescence and apoptosis in association with accumulation of DNA damage markers, PLoS ONE 8 (2013) e53168.

[6] A. Gradilone, P. Gazzaniga, D. Ribuffo, S. Scarpa, E. Cigna, F. Vasaturo, et al., Survivin, bcl-2, bax, and bcl-X gene expression in sentinel lymph nodes from melanoma patients, J. Clin. Oncol. 21 (2003) 306–312.

[7] D.C. Altieri, Survivin, cancer networks and pathway-directed drug discovery, Nat. Rev. Cancer 8 (2008) 61–70.

[8] F. Mouriaux, F. Casagrande, M.J. Pillaire, S. Manenti, F. Malecaze, J.M. Darbon, Differential expression of G1 cyclins and cyclin-dependent kinase inhibitors in normal and transformed melanocytes, Invest. Ophthalmol. Vis. Sci. 39 (1998) 876–884.

[9] M.R. Gabri, Z. Mazorra, G.V. Ripoll, C. Mesa, L.E. Fernandez, D.E. Gomez, et al., Complete antitumor protection by perioperative immunization with GM3/VSSP vaccine in a preclinical mouse melanoma model, Clin. Cancer Res. 12 (2006) 7092–7098.

[10] G.P. Dimri, X. Lee, G. Basile, M. Acosta, G. Scott, C. Roskelley, et al., A biomarker that identifies senescent human cells in culture and in aging skin in vivo, Proc. Natl. Acad. Sci. U.S.A. 92 (1995) 9363–9367.

[11] B.Y. Lee, J.A. Han, J.S. Im, A. Morrone, K. Johung, E.C. Goodwin, et al., Senescence-associated beta-galactosidase is lysosomal beta-galactosidase, Aging Cell 5 (2006) 187–195.

[12] M.M. Bradford, A rapid and sensitive method for the quantitation of microgram quantities of protein utilizing the principle of protein-dye binding, Anal. Biochem. 72 (1976) 248–254.

[13] P.J. Kim, J. Plescia, H. Clevers, E.R. Fearon, D.C. Altieri, Survivin and molecular pathogenesis of colorectal cancer, Lancet 362 (2003) 205–209.

[14] D.A. Rodriguez, J.C. Tapia, J.G. Fernandez, V.A. Torres, N. Munoz, D. Galleguillos, et al., Caveolin-1-mediated suppression of cyclooxygenase-2 via a beta-catenin-Tcf/Lef-dependent transcriptional mechanism reduced prostaglandin E2 production and survivin expression, Mol. Biol. Cell 20 (2009) 2297–2310.

[15] A. Palladini, G. Nicoletti, F. Pappalardo, A. Murgo, V. Grosso, V. Stivani, et al., In silico modeling and in vivo efficacy of cancer-preventive vaccinations, Cancer Res. 70 (2010) 7755–7763.

[16] L.E. Cabrales, J.J. Nava, A.R. Aguilera, J.A. Joa, H.M. Ciria, M.M. Gonzalez, et al., Modified Gompertz equation for electrotherapy murine tumor growth kinetics: predictions and new hypotheses, BMC Cancer 10 (2010) 589.

[17] J.M. Vicencio, L. Galluzzi, N. Tajeddine, C. Ortiz, A. Criollo, E. Tasdemir, et al., Senescence, apoptosis or autophagy? When a damaged cell must decide its path–a mini-review, Gerontology 54 (2008) 92–99.

[18] D. Hanahan, R.A. Weinberg, The hallmarks of cancer, Cell 100 (2000) 57–70.

[19] B. Ferguson, H.P. Soyer, G.J. Walker, Clinicopathological characterization of mouse models of melanoma, Methods Mol. Biol. 1267 (2015) 251–261.

[20] H. Harlin, Y. Meng, A.C. Peterson, Y. Zha, M. Tretiakova, C. Slingluff, et al., Chemokine expression in melanoma metastases associated with CD8+ T-cell recruitment, Cancer Res. 69 (2009) 3077–3085.

[21] S.R. Denmeade, J.T. Isaacs, The SERCA pump as a therapeutic target: making a "smart bomb" for prostate cancer, Cancer Biol. Ther. 4 (2005) 14–22.

[22] W. Cosme-Blanco, M.F. Shen, A.J. Lazar, S. Pathak, G. Lozano, A.S. Multani, et al., Telomere dysfunction suppresses spontaneous tumorigenesis in vivo by initiating p53-dependent cellular senescence, EMBO Rep. 8 (2007) 497–503.

[23] N.T. Van, N. Puebla-Osorio, H. Pang, M.E. Dujka, C. Zhu, DNA damage-induced cellular senescence is sufficient to suppress tumorigenesis: a mouse model, J. Exp. Med. 204 (2007) 1453–1461.

[24] J.A. Barboza, G. Liu, Z. Ju, A.K. El-Naggar, G. Lozano, p21 delays tumor onset by preservation of chromosomal stability, Proc. Natl. Acad. Sci. U.S.A. 103 (2006) 19842–19847.

[25] A.R. Choudhury, Z. Ju, M.W. Djojosubroto, A. Schienke, A. Lechel, S. Schaetzlein, et al., Cdkn1a deletion improves stem cell function and lifespan of mice with dysfunctional telomeres without accelerating cancer formation, Nat. Genet. 39 (2007) 99–105.

[26] J. Campisi, F. d'Adda di Fagagna, Cellular senescence: when bad things happen to good cells, Nat. Rev. Mol. Cell Biol. 8 (2007) 729–740.

[27] J.P. Coppe, K. Kauser, J. Campisi, C.M. Beausejour, Secretion of vascular endothelial growth factor by primary human fibroblasts at senescence, J. Biol. Chem. 281 (2006) 29568–29574.

[28] A. Krtolica, S. Parrinello, S. Lockett, P.Y. Desprez, J. Campisi, Senescent fibroblasts promote epithelial cell growth and tumorigenesis: a link between cancer and aging, Proc. Natl. Acad. Sci. U.S.A. 98 (2001) 12072–12077.

[29] M. Malumbres, M. Barbacid, To cycle or not to cycle: a critical decision in cancer, Nat. Rev. Cancer 1 (2001) 222–231.

[30] J. Massague, G1 cell-cycle control and cancer, Nature 432 (2004) 298–306.

[31] J. Bartkova, J. Lukas, M. Strauss, J. Bartek, Cyclin D1 oncoprotein aberrantly accumulates in malignancies of diverse histogenesis, Oncogene 10 (1995) 775–778.

[32] Z. Shao, Q. Bao, F. Jiang, H. Qian, Q. Fang, X. Hu, VS-5584, a novel PI3K-mTOR dual inhibitor, inhibits melanoma cell growth in vitro and in vivo, PLoS ONE 10 (2015) e0132655.

[33] Q. Yu, Y. Geng, P. Sicinski, Specific protection against breast cancers by cyclin D1 ablation, Nature 411 (2001) 1017–1021.

[34] R. Houben, J.C. Becker, A. Kappel, P. Terheyden, E.B. Brocker, R. Goetz, et al., Constitutive activation of the Ras-Raf signaling pathway in metastatic melanoma is associated with poor prognosis, J. Carcinog. 3 (2004) 6.

[35] J. Yang, S. Zaja-Milatovic, Y.M. Thu, F. Lee, R. Smykla, A. Richmond, Molecular determinants of melanoma malignancy: selecting targets for improved efficacy of chemotherapy, Mol. Cancer Ther. 8 (2009) 636–647.

[36] J. Utikal, M. Udart, U. Leiter, R.U. Peter, G. Krahn, Additional Cyclin D(1) gene copies associated with chromosome 11 aberrations in cutaneous malignant melanoma, Int. J. Oncol. 26 (2005) 597–605.

[37] E. Daveri, G. Valacchi, R. Romagnoli, E. Maellaro, E. Maioli, Antiproliferative effect of rottlerin on Sk-Mel-28 melanoma cells, Evid. Based Complement. Alternat. Med. 2015 (2015) 545838.

[38] V. Kedinger, A. Meulle, O. Zounib, M.E. Bonnet, J.B. Gossart, E. Benoit, et al., Sticky siRNAs targeting survivin and cyclin B1 exert an antitumoral effect on melanoma subcutaneous xenografts and lung metastases, BMC Cancer 13 (2013) 338.

[39] J. Georgieva, P. Sinha, D. Schadendorf, Expression of cyclins and cyclin dependent kinases in human benign and malignant melanocytic lesions, J. Clin. Pathol. 54 (2001) 229–235.

[40] M. Ozeki, D. Tamae, D.X. Hou, T. Wang, T. Lebon, D.R. Spitz, et al., Response of cyclin B1 to ionizing radiation: regulation by NF-kappaB and mitochondrial antioxidant enzyme MnSOD, Anticancer Res. 24 (2004) 2657–2663.

[41] R.J. Kelly, A. Lopez-Chavez, D. Citrin, J.E. Janik, J.C. Morris, Impacting tumor cell-fate by targeting the inhibitor of apoptosis protein survivin, Mol. Cancer 10 (2011) 35.

[42] S. Spranger, R. Bao, T.F. Gajewski, Melanoma-intrinsic beta-catenin signalling prevents anti-tumour immunity, Nature 523 (2015) 231–235.

[43] F. Azimi, R.A. Scolyer, P. Rumcheva, M. Moncrieff, R. Murali, S.W. McCarthy, et al., Tumor-infiltrating lymphocyte grade is an independent predictor of sentinel lymph node status and survival in patients with cutaneous melanoma, J. Clin. Oncol. 30 (2012) 2678–2683.

[44] A.H. Rossi, A. Farias, J.E. Fernandez, H.R. Bonomi, F.A. Goldbaum, P.M. Berguer, Brucella spp. lumazine synthase induces a TLR4-mediated protective response against B16 melanoma in mice, PLoS ONE 10 (2015) e0126827.

[45] J. Galon, A. Costes, F. Sanchez-Cabo, A. Kirilovsky, B. Mlecnik, C. Lagorce-Pages, et al., Type, density, and location of immune cells within human colorectal tumors predict clinical outcome, Science 313 (2006) 1960–1964.

[46] F. Pages, A. Berger, M. Camus, F. Sanchez-Cabo, A. Costes, R. Molidor, et al., Effector memory T cells, early metastasis, and survival in colorectal cancer, N. Engl. J. Med. 353 (2005) 2654–2666.

[47] C.M. Koebel, W. Vermi, J.B. Swann, N. Zerafa, S.J. Rodig, L.J. Old, et al., Adaptive immunity maintains occult cancer in an equilibrium state, Nature 450 (2007) 903–907.

[48] G.P. Dunn, L.J. Old, R.D. Schreiber, The three Es of cancer immunoediting, Annu. Rev. Immunol. 22 (2004) 329–360.

[49] M.J. Smyth, G.P. Dunn, R.D. Schreiber, Cancer immunosurveillance and immunoediting: the roles of immunity in suppressing tumor development and shaping tumor immunogenicity, Adv. Immunol. 90 (2006) 1–50.

[50] R.R. Ji, S.D. Chasalow, L. Wang, O. Hamid, H. Schmidt, J. Cogswell, et al., An immune-active tumor microenvironment favors clinical response to ipilimumab, Cancer Immunol. Immunother. 61 (2012) 1019–1031.

[51] S.J. Elledge, Cell cycle checkpoints: preventing an identity crisis, Science 274 (1996) 1664–1672.

[52] L.H. Hartwell, M.B. Kastan, Cell cycle control and cancer, Science 266 (1994) 1821–1828.

[53] M.C. Yang, S.U. Choi, W.S. Choi, S.Y. Kim, K.R. Lee, Guaiane sesquiterpene lactones and amino acid-sesquiterpene lactone conjugates from the aerial parts of Saussurea pulchella, J. Nat. Prod. 71 (2008) 678–683.

[54] G. Negrin, J.L. Eiroa, M. Morales, J. Triana, J. Quintana, F. Estevez, Naturally occurring asteriscunolide A induces apoptosis and activation of mitogen-activated protein kinase pathway in human tumor cell lines, Mol. Carcinog. 49 (2010) 488–499.

[55] K. Lesiak, K. Koprowska, I. Zalesna, D. Nejc, M. Duchler, M. Czyz, Parthenolide, a sesquiterpene lactone from the medical herb feverfew, shows anticancer activity against human melanoma cells in vitro, Melanoma Res. 20 (2010) 21–34.

[56] J. Triana, J.L. Eiroa, J.J. Ortega, F. Leon, I. Brouard, F. Torres, et al., Sesquiterpene lactones from Gonospermum gomerae and G. fruticosum and their cytotoxic activities, J. Nat. Prod. 71 (2008) 2015–2020.

[57] F.F. Arantes, L.C. Barbosa, E.S. Alvarenga, A.J. Demuner, D.P. Bezerra, J.R. Ferreira, et al., Synthesis and cytotoxic activity of alpha-santonin derivatives, Eur. J. Med. Chem. 44 (2009) 3739–3745.

[58] Y. Yan, G.X. Chou, W. Hui, J.H. Chu, W.F. Fong, Z.L. Yu, Effects of sesquiterpenes isolated from largehead atractylodes rhizome on growth, migration, and differentiation of B16 melanoma cells, Integr. Cancer Ther. 10 (2011) 92–100.

[59] P. Pratheeshkumar, G. Kuttan, Effect of vernolide-A, a sesquiterpene lactone from Vernonia cinerea L., on cell-mediated immune response in B16F-10 metastatic melanoma-bearing mice, Immunopharmacol. Immunotoxicol. 33 (2011) 533–538.

[60] G. Kuttan, P. Pratheeshkumar, K.A. Manu, R. Kuttan, Inhibition of tumor progression by naturally occurring terpenoids, Pharm. Biol. 49 (2011) 995–1007.

[61] P. Pratheeshkumar, G. Kuttan, Antimetastatic potential of vernolide-A, a sesquiterpenoid from Vernonia cinerea L, Hum. Exp. Toxicol. 31 (2012) 66–80.